

Accurate fit of the two lowest excitedstate potentialenergy surfaces for doublet HeH2 +

Alfredo Aguado, Cristina Suárez, and Miguel Paniagua

Citation: *The Journal of Chemical Physics* **98**, 308 (1993); doi: 10.1063/1.464676

View online: <http://dx.doi.org/10.1063/1.464676>

View Table of Contents: <http://scitation.aip.org/content/aip/journal/jcp/98/1?ver=pdfcov>

Published by the [AIP Publishing](#)

Articles you may be interested in

Accurate intermolecular ground-state potential-energy surfaces of the HCCH–He, Ne, and Ar van der Waals complexes

J. Chem. Phys. **123**, 014309 (2005); 10.1063/1.1947189

Ground and lower excitedstate discrete a b i n i t i o electronic potentialenergy surfaces for doublet HeH2 +a)

J. Chem. Phys. **70**, 2748 (1979); 10.1063/1.437861

Potential energy surface for the collinear reaction of Ne and HeH

J. Chem. Phys. **69**, 2264 (1978); 10.1063/1.436790

Modified AtomsinMolecules Model for Predicting Diatomic Ground and ExcitedState PotentialEnergy Curves. I. LiH, BeH, and BH

J. Chem. Phys. **43**, 3654 (1965); 10.1063/1.1696533

Molecular Orbital Studies of Excited States of HeH

J. Chem. Phys. **39**, 1464 (1963); 10.1063/1.1734465



Accurate fit of the two lowest excited-state potential-energy surfaces for doublet HeH_2^+

Alfredo Aguado, Cristina Suárez, and Miguel Paniagua

Departamento de Química Física, Facultad de Ciencias C-XIV, Universidad Autónoma de Madrid, 28049 Madrid, Spain

(Received 7 July 1992; accepted 15 September 1992)

Diabatic potential-energy functions for the two lowest excited states of the doublet HeH_2^+ system which fit published *ab initio* data [McLaughlin and Thompson, J. Chem. Phys. **70**, 2748 (1979)] at a quantitative level have been obtained, similar to that obtained previously for the ground state (root-mean-square error about 1 kcal/mol), and without any quantity of *ad hoc* character, preserving the accuracy of the *ab initio* points. The corresponding adiabatic potential-energy functions are obtained by solving a 2×2 determinant that uses the diabatic energies and an interaction term fitted to the lowest eigenvalue to obtain a global root mean square as low as possible (0.93 kcal/mol). The lowest adiabatic potential-energy function satisfies the criteria needed to be used in full three-dimensional scattering calculations for the collisionally-induced predissociation charge-exchange reaction $\text{He}^+ + \text{H}_2 \rightarrow \text{He} + \text{H}^+ + \text{H}$ and, using the ground-state potential-energy surface also, the collision-induced dissociation reaction $\text{H}_2^+(v) + \text{He} \rightarrow \text{He} + \text{H}^+ + \text{H}$ and the exoergic reaction $\text{He}^+ + \text{H}_2 \rightarrow \text{HeH}^+ + \text{H}$.

I. INTRODUCTION

The three-electron HeH_2^+ system is one of the most studied ion-molecule systems and it is considered as a model system of the nuclear dynamics of elementary chemical reactions involving excited electronic states, because theoretical calculations of both the potential-energy surface (PES) and the scattering problem are expected to be accurate and there are many experimental studies with sufficient resolution for comparison with theory. A summary of experimental work on reactive scattering in $\text{He} + \text{H}_2^+$ may be found in recent papers of Pollard *et al.*¹ and a review of the experimental work on $\text{He}^+ + \text{H}_2$ collisions is given by Pollack and Hahn.²

Ab initio PES calculations have been carried out for the ground state and several excited states for the HeH_2^+ system in collinear^{3,4} and three-dimensional geometries.⁵⁻⁸ In addition, diatomics-in-molecules (DIM) PES have been developed for this system.^{9,10}

Scattering calculations for $\text{He} + \text{H}_2^+$ have been performed by classical trajectory and quantum-mechanical methods; the early work has been reviewed by Tiernan and Lifshitz¹¹ but from the date of the review many other recent work have been published.¹²⁻¹⁸ However, except for the work done by Gislason *et al.*¹⁵ on the collision-induced dissociation (CID) process based on DIM surfaces,⁹ all the scattering calculations have been restricted to the ground PES of HeH_2^+ for the reaction $\text{He} + \text{H}_2^+ \rightarrow \text{HeH}^+ + \text{H}$. This is not a surprising fact if we consider that, from the publication of the accurate *ab initio* configuration-interaction energies for the four lowest doublet HeH_2^+ by McLaughlin and Thompson,⁶ more than one decade ago, no fits of the excited-state PES and only two fits of the ground-state PES to analytic functions have appeared^{14,19} with root-mean-square (rms) errors of 1.6 kcal/mol (526 points used in the fit)¹⁴ and 0.7 kcal/mol (551 points used in the fit),¹⁹ respectively.

In this paper we present the first fit of the two lowest excited-states of the doublet HeH_2^+ system using the configuration-interaction energies in the corresponding diabatic analysis made by McLaughlin and Thompson.⁶ These two states intersect and, because both states are $^2A'$ in C_s symmetry, the intersection will be avoided at other than C_{2v} configurations where these two states are 2A_1 and 2B_2 . Therefore, we produce the corresponding adiabatic PES in C_s symmetry by solving a 2×2 determinant that uses the diabatic energies and an interaction term fitted to the lowest eigenvalue to obtain a global root mean square as low as possible. Finally, several properties of the PES thus obtained are compared with those obtained by Hopper⁵ using *ab initio* multiconfiguration self-consistent-field (MCSCF) procedure.

II. THE DIABATIC POTENTIALS

The HeH_2^+ diabatic potentials corresponding to the two lowest excited states are fitted by means of the same global fitting procedure used for the ground state.¹⁹ This procedure is based on the many-body expansion²⁰

$$V_{ABC} = \sum_A V_A^{(1)} + \sum_{AB} V_{AB}^{(2)}(R_{AB}) + V_{ABC}^{(3)}(R_{AB}, R_{AC}, R_{BC}), \quad (1)$$

where the summations run over all the terms of a given type and where $V_A^{(1)}$ is the energy of atom A in its appropriate electronic state; usually, we adopt $\sum_A V_A^{(1)} = 0$ for all the atoms in their ground state. $V_{AB}^{(2)}$ is the two-body energy, that is expressed using a polynomial form¹⁹

$$V_{AB}^{(2)} = \frac{c_0 e^{-\alpha_{AB} R_{AB}}}{R_{AB}} + \sum_{i=1}^N c_i \rho_{AB}^i, \quad (2)$$

and the polynomial Rydberg type variables²¹ ρ are given by

TABLE I. Parameters (in atomic units) of the two-body term $V_{\text{HH}}^{(2)}$ corresponding to $A^2\Sigma_u^+$ state of the H₂⁺.

i	c_i
0	0.137 341 352(+01)
1	0.440 786 333(+00)
2	0.579 577 189(+00)
α_{HH}^{+}	0.623 321 470(+00)
$\beta_{\text{HH}}^{(2)+}$	0.107 210 690(+01)

TABLE II. Parameters (in atomic units) of the two-body term $V_{\text{HeH}}^{(2)}$ corresponding to $X^2\Sigma^+$ state of the HeH.

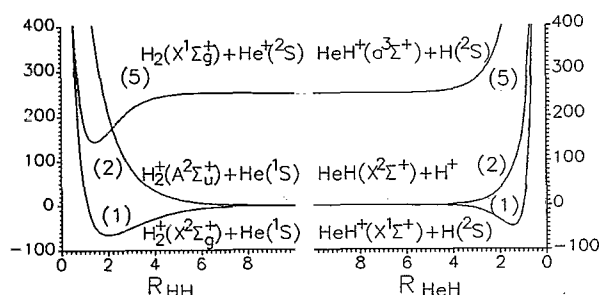
i	c_i
0	0.124 626 771(+01)
1	0.126 174 791(-01)
2	0.121 575 753(+01)
α_{HeH}	0.194 754 840(+01)
$\beta_{\text{HeH}}^{(2)}$	0.114 565 862(+01)

TABLE III. Parameters (in atomic units) of the two-body term $V_{\text{HH}}^{(2)}$ corresponding to $X^1\Sigma_g^+$ state of the H₂.

i	c_i
0	0.425 235 796(+00)
1	-0.144 114 114(+01)
α_{HH}	0.389 722 415(+00)
$\beta_{\text{HH}}^{(2)}$	0.125 818 395(+01)

TABLE IV. Parameter (in atomic units) of the two-body term $V_{\text{HeH}}^{(2)}$ corresponding to $a^3\Sigma^+$ state of the HeH⁺.

i	c_i
0	0.233 380 002(+01)
α_{HeH}	0.847 572 492(+00)

FIG. 1. Asymptotic cuts of the ground-state surface, code number (1), and the two lowest excited states, code numbers (2) and (5), of HeH₂⁺. The left side displays the diatomic energy in the reactants region which results when a He nucleus is far apart; the right side gives the diatomic energy in the products region which results when a H nucleus is far apart. This figure was generated using the parameters given in Tables I–IV (this paper) for the excited states and the parameters given in Table IV (Ref. 19) for the ground state.

$$\rho_{AB} = R_{AB} e^{-\beta_{AB}^{(l)} R_{AB}}, \quad l=2 \text{ or } 3. \quad (3)$$

The linear parameters c_i , $i=0,1,\dots,N$ and the nonlinear parameters α_{AB} and $\beta_{AB}^{(2)}$ are determined by fitting the *ab initio* values corresponding to diabatic states of the diatomic fragments (plus separated atom at large enough distance) computed with the same basis set as for the triatomic system and using the same *ab initio* procedure.

In Tables I–IV we present the parameters obtained for the fits of the diatomic fragments needed to fit the two lowest diabatic excited states of the HeH₂⁺, that correspond to code numbers (2) and (5) in the diabatic ordering of eigenvalues given by McLaughlin and Thompson.⁶ Code number (2) refers to H₂⁺(A²Σ_u⁺) + He(1S) in the reactants channel and HeH(X²Σ⁺) + H⁺ in the products channel. Code number (5) corresponds to H₂(X¹Σ_g⁺) + He⁺(2S) in the reactants channel and HeH⁺(a³Σ⁺) + H(2S) in the products channel.

There are few calculated *ab initio* energies of the HeH₂⁺ for the separated atom plus diatomic fragments. However, except for the code (5) products channel excited state where no *ab initio* points are presented, these energies are enough for the aim of the global triatomic fit. We avoid the lack of *ab initio* energies for the code (5) products channel excited state by using the next two points for the fit: (i) the asymptotic limit at $R_{\text{HeH}}=100$ a.u. of the corresponding code (5) reactants channel excited-state and (ii) the energy at $R_{\text{HeH}}=1$ a.u. obtained by exponential extrapolation of the global code (5) triatomic data. Moreover, we use for this fit only the first term in Eq. (2) because of the repulsive nature of this potential,²² and we optimize independently the corresponding parameters in Table IV to obtain a good rms value in the subsequent global triatomic fit.

Figure 1 shows the projection of the ground-state sur-

TABLE V. Parameters (in atomic units) of the three-body term $V_{\text{HeHH}}^{(3)}$ corresponding to (2) ²A' diabatic excited state of the HeH₂⁺. By symmetry $d_{ijk}=d_{jik}$.

ijk	d_{ijk}	ijk	d_{ijk}
1 0 1	-0.274 315 093(+01)	0 2 3	0.615 497 062(+02)
1 1 0	-0.168 370 459(+01)	4 0 1	0.488 763 627(+03)
1 1 1	-0.386 358 216(+02)	4 1 0	-0.150 888 766(+04)
2 0 1	0.107 239 761(+02)	0 1 4	0.341 582 491(+03)
2 1 0	0.434 916 605(+01)	2 2 2	0.465 142 287(+04)
0 1 2	0.384 681 533(+02)	3 1 2	-0.254 094 051(+04)
2 1 1	-0.104 038 580(+02)	3 2 1	-0.204 491 669(+04)
1 1 2	0.173 339 027(+03)	1 2 3	0.160 674 604(+04)
2 0 2	-0.503 465 955(+02)	3 0 3	0.676 202 548(+02)
2 2 0	-0.421 003 524(+03)	3 3 0	0.401 097 195(+03)
3 0 1	-0.150 682 020(+03)	4 1 1	0.574 474 883(+03)
3 1 0	0.310 639 422(+03)	1 1 4	-0.260 001 919(+04)
0 1 3	-0.186 673 585(+03)	4 0 2	-0.158 637 012(+03)
2 1 2	-0.877 758 743(+03)	4 2 0	-0.663 234 612(+03)
2 2 1	0.339 553 954(+03)	0 2 4	0.135 772 754(+03)
3 1 1	0.502 203 725(+03)	5 0 1	-0.607 214 960(+03)
1 1 3	0.694 700 977(+03)	5 1 0	0.218 661 888(+04)
3 0 2	0.217 739 410(+03)	0 1 5	-0.176 001 915(+03)
3 2 0	0.752 523 543(+03)		
$\beta_{\text{HH}}^{(3)+}$	0.942 851 780(+00)	$\beta_{\text{HeH}}^{(3)+}$	0.105 286 140(+01)

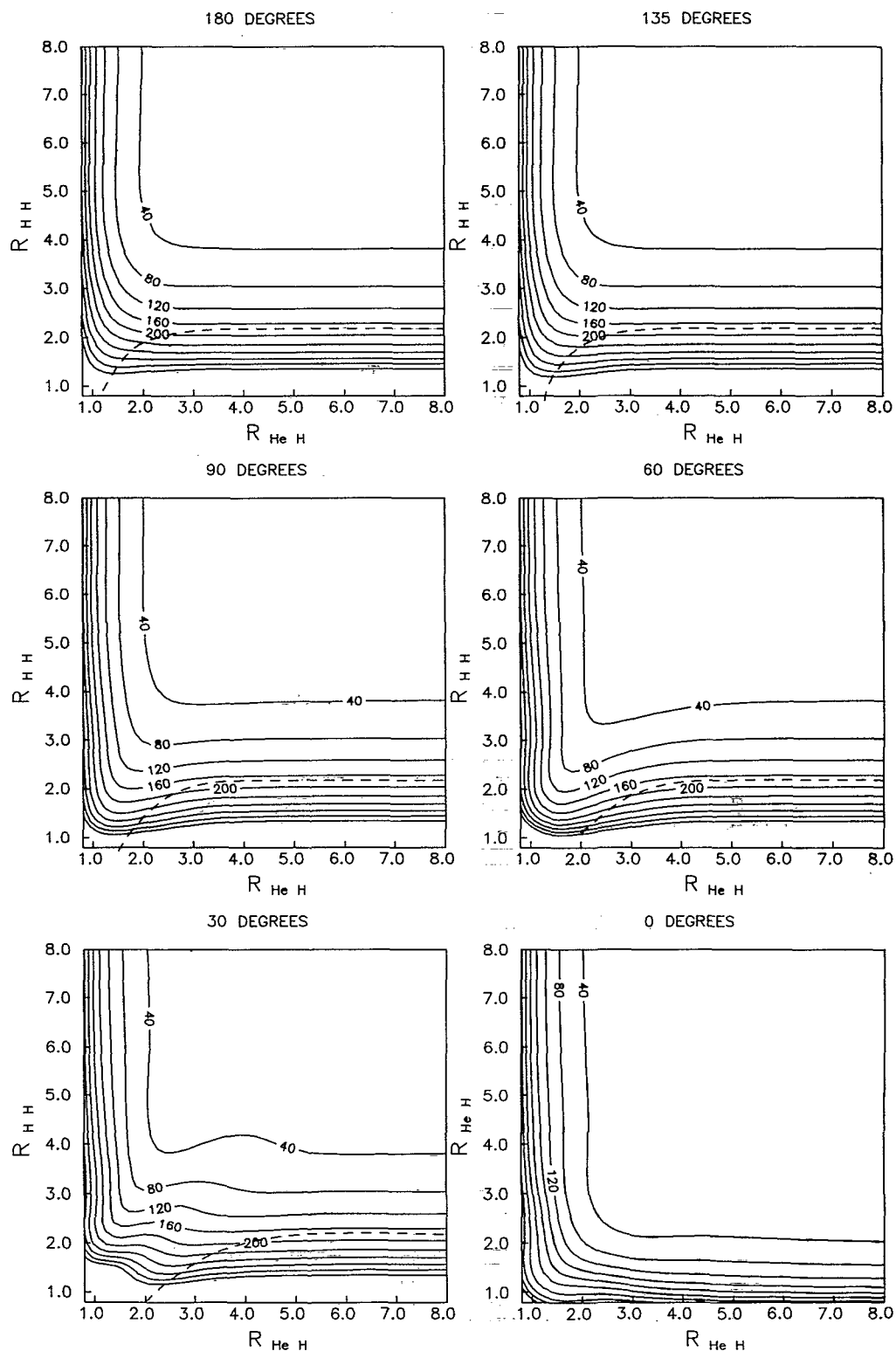


FIG. 2. Potential contours of the HeH_2^+ interaction potential for the $(2) {}^2A'$ diabatic excited state. For each contour map one internal bond angle is fixed, as indicated at the top of each panel. The solid curves are contours of the interaction potential corresponding to 40, 80, 120, 160, 200, 240, 280, 320, 360, and 400 kcal/mol with respect to the zero energy fixed at the separated atoms. The dashed curves indicate at each panel the crossing line with the $(5) {}^2A'$ diabatic excited state. All the interatomic distances are in atomic units.

face [code (1) in the diabatic ordering given by McLaughlin and Thompson⁶ which was fitted in a previous paper¹⁹] and the two diabatic excited-state surfaces of HeH₂⁺ (fitted here, see Tables I–IV) on their asymptotic diatomic limits. The left side of Fig. 1 gives the result when the He nucleus is pulled away (reactants channel), while the right side presents the limit when an H nucleus is removed (products channel). From Fig. 1 it is clear that the reagents in the exothermic reaction (−190.8 kcal/mol) He⁺ + H₂ → HeH⁺ + H, for H₂ in a low vibrational state, correlate with the code (5) excited-state potential, while the products correlate with the code (1) ground-state potential.^{22,23} Moreover, Fig. 1 reveals an important surface crossing²² that is suggestive of a collisional predissociation process. Dissociative charge-exchange reaction He⁺ + H₂ → He + H⁺ + H may be produced through the interaction of the code (2) excited state with the code (5) excited state in the reactants channel.

The three-body term $V_{ABC}^{(3)}$ of the potential in Eq. (1) is also expressed as a polynomial of order M in the same Rydberg type variables²¹ ρ_{AB} , ρ_{AC} , and ρ_{BC} [see Eq. (3) with $l=3$]:

$$V_{ABC}^{(3)}(R_{AB}, R_{AC}, R_{BC}) = \sum_{i,j,k} d_{ijk} \rho_{AB}^i \rho_{AC}^j \rho_{BC}^k \quad (4)$$

where some constraints must be fulfilled to ensure a good behavior of the whole potential.¹⁹ As the system under consideration has two atoms of the same type (AB_2 system), there is an evident symmetry in Eq. (4) that implies the additional constraints: $d_{ijk} = d_{jik}$ and $\beta_{AB}^{(3)} = \beta_{AB'}^{(3)}$. The same polynomial form of Eq. (4) has been used, without the nonlinear parameters $\beta_{AB}^{(3)}$, to fit the MgFH PES.²⁴

For the (2) ²A' diabatic excited state of the HeH₂⁺, the number of calculated *ab initio* points is lower than the calculated for the ground state.⁶ Moreover, we fit all the points corresponding to internuclear distances greater than 1.4a₀, because of the high-energy values for lower internuclear distances that are well described by the short-range term of the two-body potentials [the first term in Eq. (2)]. Thus, we use 371 calculated energies for the fit. In Table V we give the parameters of the three-body term for the (2) ²A' diabatic excited state with order $M=6$ [37 linear parameters and 2 nonlinear parameters, see Eq. (4)] and rms value of 1.08 kcal/mol and a maximum deviation of 6.45 kcal/mol corresponding to a point at short internuclear distances with more than 300 kcal/mol with respect to the zero energy that we adopt to be the energy of the three separated atoms at their ground states: He(¹S) + H⁺ + H(²S).

Using the preceding fit we generate contour maps of the PES for the (2) ²A' diabatic excited state of the HeH₂⁺, that we can see in Fig 2. For each contour map the internal bond angle is fixed to 180°, 135°, 90°, 60°, 30°, and 0°. The dashed curves in Fig. 2 indicate the crossing line with the (5) ²A' diabatic excited state of the HeH₂⁺. In fact, the contour map corresponding to 135° is totally interpolated because there are no calculated *ab initio* points for this internal bond angle. As we can see in Fig. 2, all the maps

TABLE VI. Parameters (in atomic units) of the three-body term $V_{\text{HeHH}^+}^{(3)}$ corresponding to (5) ²A' diabatic excited state of the HeH₂⁺. By symmetry $d_{ijk} = d_{jik}$.

ijk	d_{ijk}	ijk	d_{ijk}
1 0 1	−0.259 637 382(+02)	0 2 3	0.248 584 055(+04)
1 1 0	−0.406 667 831(+01)	4 0 1	0.394 808 800(+03)
1 1 1	0.421 693 605(+03)	4 1 0	0.137 918 693(+05)
2 0 1	0.107 149 848(+03)	0 1 4	0.132 543 028(+04)
2 1 0	−0.305 989 929(+02)	2 2 2	0.454 910 086(+05)
0 1 2	0.206 034 605(+03)	3 1 2	0.224 888 109(+04)
2 1 1	0.317 653 883(+04)	3 2 1	−0.190 402 300(+05)
1 1 2	−0.394 741 227(+04)	1 2 3	0.674 499 843(+04)
2 0 2	−0.641 770 150(+03)	3 0 3	0.149 718 500(+04)
2 2 0	0.669 852 909(+03)	3 3 0	−0.795 799 713(+05)
3 0 1	0.284 616 500(+03)	4 1 1	−0.116 954 025(+06)
3 1 0	−0.688 199 682(+04)	1 1 4	−0.109 340 567(+05)
0 1 3	−0.766 873 523(+03)	4 0 2	0.143 975 633(+05)
2 1 2	−0.103 565 467(+05)	4 2 0	0.529 767 302(+05)
2 2 1	−0.310 682 817(+05)	0 2 4	−0.273 915 971(+04)
3 1 1	0.286 292 903(+05)	5 0 1	−0.948 150 378(+04)
1 1 3	0.114 571 871(+05)	5 1 0	0.431 573 910(+05)
3 0 2	−0.418 830 340(+04)	0 1 5	−0.853 329 543(+03)
3 2 0	0.163 825 516(+05)		
$\beta_{\text{HH}^+}^{(3)}$	0.925 627 190(+00)	$\beta_{\text{HeH}^+}^{(3)}$	0.132 573 135(+01)

present a correct behavior at short, intermediate, and long range of the potential. Moreover, the fitting procedure does not give rise to spurious features and the functions adopted here present a simple global form with simple derivatives. Thus, this PES satisfies the criteria needed for use in full three-dimensional scattering calculations.

As for the diatomic fragments, the number of *ab initio* calculated energies for the code (5) diabatic excited state is lower than the calculated energies for the code (2) diabatic excited state. Thus, we use all the calculated points (240) to fit the three-body term of the (5) ²A' diabatic excited state of the HeH₂⁺. In Table VI we give the parameters of the three-body term for the (5) ²A' diabatic excited state with order $M=6$ [with the same number of parameters than for the (2) ²A' diabatic excited state] and rms value of 1.03 kcal/mol and a maximum deviation of 5.99 kcal/mol corresponding to a point with very high energy with respect to the zero energy (the separated atoms at their ground states). For this excited state we must take into account that $\sum_A V_A^{(1)} = 0.4003$ hartree (251.2 kcal/mol) corresponding to He⁺(²S) + H(²S) + H(²S).

Figure 3 shows contour maps of the PES for the (5) ²A' diabatic excited state of HeH₂⁺, generated using the preceding fit. For each contour map the internal bond angle is fixed to 180°, 135°, 90°, 60°, 30°, and 0°. The dashed curves in Fig. 3 indicate the crossing line with the (2) ²A' diabatic excited state of the HeH₂⁺. As for Fig. 2, the contour map corresponding to 135° is totally interpolated because there are no calculated *ab initio* points for this internal bond angle. Also in this case, all the maps present a correct behavior at short, intermediate, and long range of the potential; thus, also satisfying the criteria needed for use in full three-dimensional scattering calculations.

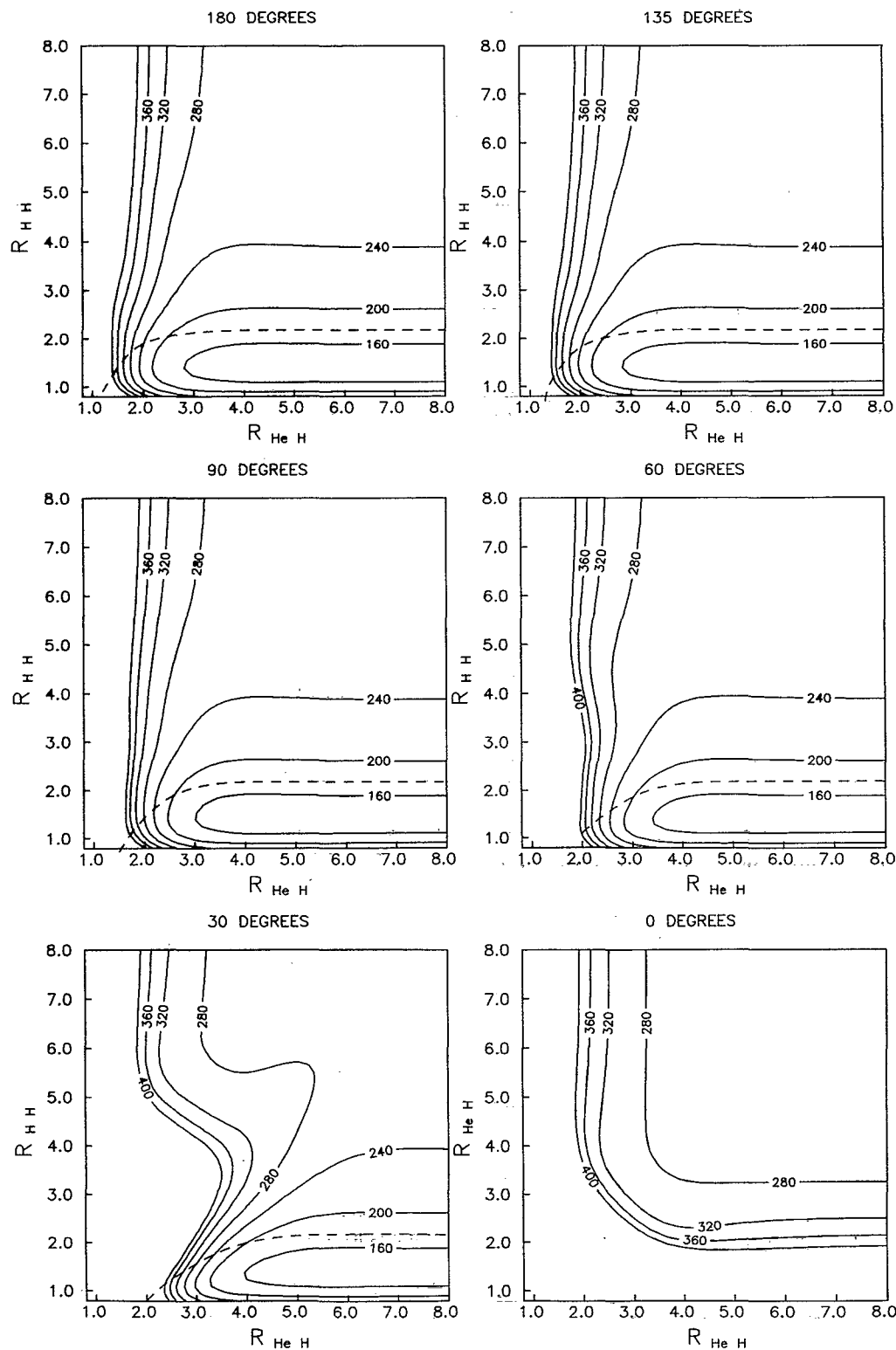


FIG. 3. Potential contours of the HeH_2^+ interaction potential for the $(5) \ ^2A'$ diabatic excited state. For each contour map one internal bond angle is fixed, as indicated at the top of each panel. The solid curves are contours of the interaction potential corresponding to 160, 200, 240, 280, 320, 360, and 400 kcal/mol with respect to the zero energy fixed at the separated atoms. The dashed curves indicate at each panel the crossing line with the $(2) \ ^2A'$ diabatic excited state. All the interatomic distances are in atomic units.

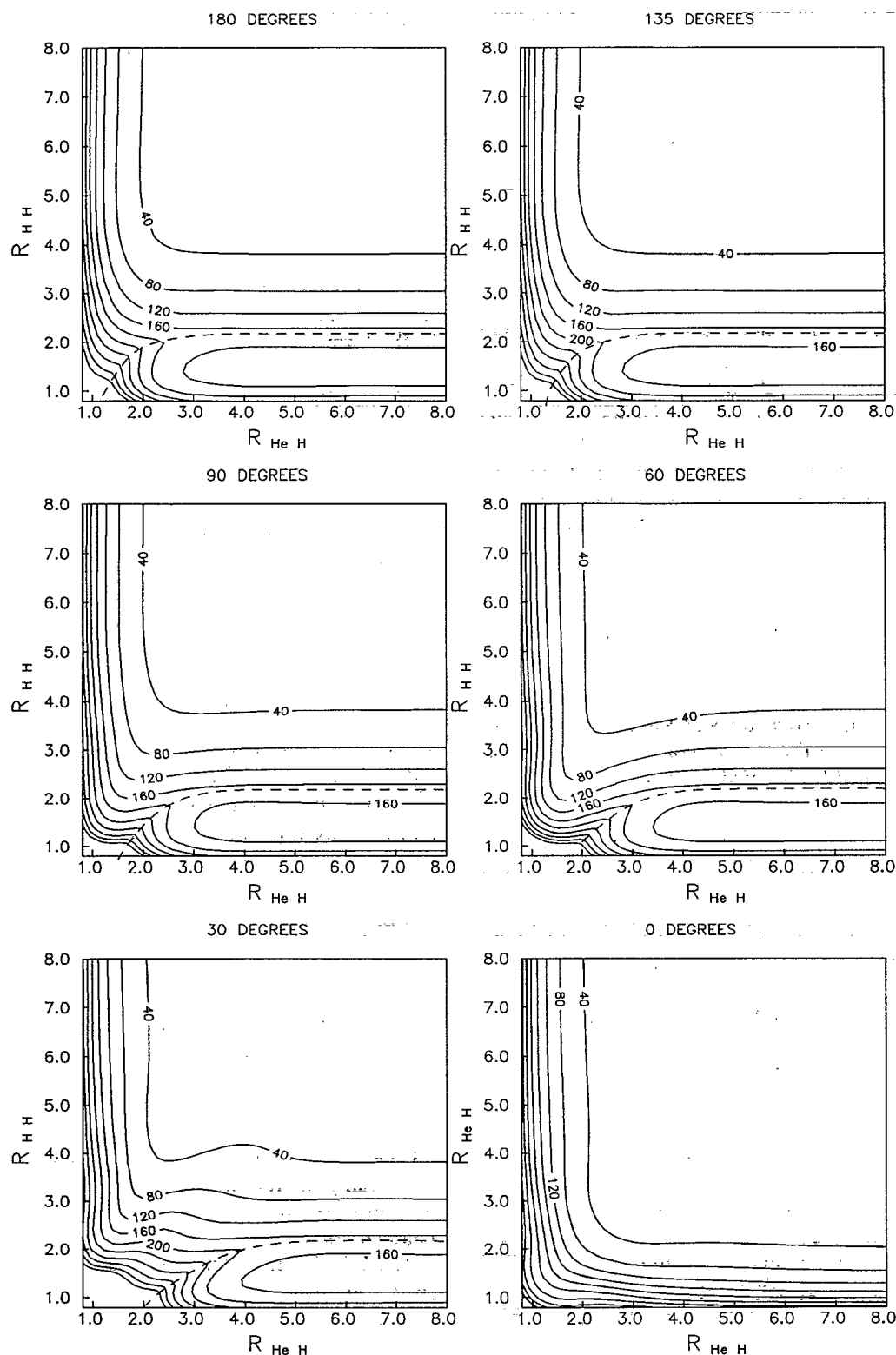


FIG. 4. Potential contours of the HeH_2^+ interaction potential for the $2\ ^2A'$ adiabatic excited state. For each contour map one internal bond angle is fixed, as indicated at the top of each panel. The solid curves are contours of the interaction potential corresponding to 40, 80, 120, 160, 200, 240, 280, 320, 360, and 400 kcal/mol with respect to the zero energy fixed at the separated atoms. The dashed curves indicate at each panel the crossing line between the $(2)\ ^2A'$ and $(5)\ ^2A'$ diabatic excited states. All the interatomic distances are in atomic units.

TABLE VII. Properties comparison in the minimum of the 2²A' adiabatic excited state of the HeH₂⁺. All the results are given in atomic units except the wavelength for the transition 2²A₁ → 1²A₁ which is given in nanometers.

	Hopper		This paper	
	C _{2v}	C _{∞v}	C _{2v}	C _{∞v}
R _{HH}	1.40	1.40	1.421	1.416
R _{He⁺-H₂}	4.917	5.73	4.448	5.278
E _T ^e	-3.1537 (3 MC)	-3.1510 (3 MC)	-3.1725	-3.1709
	-3.1707 (7 MC)			
k _{He⁺-H₂}	0.004 07	0.001 67	0.004 19	0.002 19
D _{He⁺-H₂} ^e	0.003 18	0.000 47	0.002 98	0.001 35
λ(2 ² A ₁ → 1 ² A ₁)	154.3		152.0	

III. THE ADIABATIC POTENTIALS

PES near intersections have been discussed in detail very recently.^{25,26} As stated by Ruedenberg *et al.*, the two intersecting adiabatic states ψ_1 and ψ_2 can be expressed as linear combinations of two *arbitrary* diabatic orthogonal states ϕ_1 and ϕ_2 in the function space that is complementary to the space spanned by all other eigenstates ψ_n ($n \geq 3$), whose energies E_3, E_4, \dots are assumed to be nondegenerate with E_1 and E_2 . Then, the adiabatic energies E_1 and E_2 (hereafter referred to as E_{\pm}) are given in terms of the diabatic energies E_{11} and E_{22} :

$$E_{\pm} = \frac{1}{2} \{ (E_{11} + E_{22}) \pm [(E_{11} - E_{22})^2 + 4E_{12}^2]^{1/2} \}. \quad (5)$$

The advantage in using the diabatic states instead of the adiabatic ones is that the energy variation is smoother. Thus, it is easier to fit the diabatic states and to produce the adiabatic energies using Eq. (5). According to Eq. (5) the intersection is defined by the two crossing conditions²⁶

$$E_{11} = E_{22}, \quad (6)$$

$$E_{12} = 0. \quad (7)$$

To obtain the interaction term E_{12} in Eq. (5) we take into account the topographic characteristics near the intersection. In our problem, the two excited states considered belong to the same irreducible representation for collinear geometries (both belong to Σ in $C_{\infty v}$) and for arbitrary geometries (both belong to A' in C_s), while one of them belongs to A_1 and the other one belongs to B_2 for perpendicular geometries (C_{2v}). Therefore, the intersection coordinate subspace²⁶ is a line in C_s and also in C_{2v} . Therefore, bearing in mind that the electronic Hamiltonian is totally symmetric (E_{11} and E_{22} belonging to A_1 irreducible representation in C_{2v}) and that the interaction term is asymmetric (E_{12} belonging to B_2 irreducible representation in C_{2v}), the following symmetry requirements must be fulfilled:

$$E_{ii}(R_{\text{HeH}}, R_{\text{HeH}'}, R_{\text{HH}'}) = E_{ii}(R_{\text{HeH}'}, R_{\text{HeH}}, R_{\text{HH}'}), \quad i = 1, 2 \quad (8)$$

$$E_{12}(R_{\text{HeH}}, R_{\text{HeH}'}, R_{\text{HH}'}) = -E_{12}(R_{\text{HeH}'}, R_{\text{HeH}}, R_{\text{HH}'}). \quad (9)$$

The first condition [Eq. (8)] is fulfilled by the diabatic energies, fitted in the preceding section, due to the equivalent condition $d_{ijk} = d_{jik}$ for the fitting coefficients as indi-

cated in Tables V and VI and in Sec. II. To fulfill the second condition [Eq. (9)] we choose the interaction term in the form

$$\begin{aligned} E_{12}(R_{\text{HeH}}, R_{\text{HeH}'}, R_{\text{HH}'}) \\ = C_{12} R_{\text{HH}'} e^{-\beta_1 R_{\text{HH}'}} (R_{\text{HeH}} e^{-\beta_2 R_{\text{HeH}}} - R_{\text{HeH}'} e^{-\beta_2 R_{\text{HeH}'} }). \end{aligned} \quad (10)$$

Another functional form for the interaction term has been proposed in the literature for the H₂F (Ref. 27) [but does not fulfill the symmetry requirement of Eq. (9)] and H₂O molecules (Ref. 28). We think that the function proposed here [Eq. (10)] is flexible enough for fitting the 2²A' adiabatic excited state of the HeH₂⁺. To this end, the lowest eigenvalue, which is E_- in Eq. (5), was then fitted to all data on the lowest energy sheet of the two-valued PES. The optimum values found for the interaction term parameters (given in atomic units) of this last fit are $C_{12} = 13.499\,870\,71$, $\beta_1 = 3.528\,598\,08$, and $\beta_2 = 0.859\,824\,61$ and the rms value of 0.93 kcal/mol with a maximum deviation of 3.92 kcal/mol in a point of the PES with very high energy (about 275 kcal/mol) with respect to the zero energy.

In Fig. 4 we show the contour maps of the PES for the 2²A' adiabatic excited state of the HeH₂⁺, obtained using the preceding fit for the interaction term and the corresponding fits of the diabatic excited states. For each contour map the internal bond angle is fixed to 180°, 135°, 90°, 60°, 30°, and 0°. The dashed curves in Fig. 4 indicate the crossing line between the diabatic excited states of the HeH₂⁺ considered in Sec. II. We can see from Fig. 4 that all the maps present a correct behavior.

Finally, as for the ground state,¹⁹ the 2²A' adiabatic excited state presents a minimum located at the reactants channel that, in this case, corresponds to He⁺(²S) + H₂(X¹Σ_g⁺). In Table VII we compare the well location for C_{2v} and $C_{\infty v}$ geometries with Hopper's results.⁵ We can see that the greater difference is in the distance $R_{\text{He}^+-\text{H}_2}$. The force constant $k_{\text{He}^+-\text{H}_2}$ and the dissociation energy $D_{\text{He}^+-\text{H}_2}^e$ are more similar to the results of Hopper for C_{2v} than for $C_{\infty v}$ symmetries. However, the wavelength for the transition between the first excited state and the ground state is very similar indicating that the relative error in the

7 MC (seven configurations MCSCF) Hopper energies (E_T^c) is as low as the energies of McLaughlin and Thompson.⁶

IV. CONCLUSIONS

An accurate fit of the PES corresponding to the two lowest diabatic excited states and the first adiabatic excited state for the HeH_2^+ , to an analytic function satisfying the criteria²⁹ needed for use in three-dimensional scattering calculations, using the accurate CI energy values obtained by McLaughlin and Thompson more than one decade ago, has been made. All the subroutines (FORTRAN-77) to generate all the PES presented here and their first partial derivatives are available from the authors upon request.

ACKNOWLEDGMENTS

Financial support from the Comisión para la Investigación Científica y Técnica (CICYT, No. PS-88-0013, Spain) is gratefully acknowledged.

¹J. E. Pollard, L. K. Johnson, D. A. Lichtin, and R. B. Cohen, *J. Chem. Phys.* **95**, 4877 (1991); J. E. Pollard, L. K. Johnson and R. B. Cohen, *ibid.* **95**, 4894 (1991).

²E. Pollack and Y. Hahn, *Adv. At. Mol. Phys.* **22**, 243 (1986).

³P. J. Brown and E. F. Hayes, *J. Chem. Phys.* **55**, 922 (1971).

⁴C. Edminton, J. Doolittle, K. Murphy, K. C. Tang, and W. Wilson, *J. Chem. Phys.* **52**, 3419 (1970).

⁵D. G. Hopper, *Int. J. Quantum Chem. Symp.* **12**, 305 (1978); *J. Chem. Phys.* **73**, 3289 (1980); **73**, 4528 (1980).

⁶D. R. McLaughlin and D. L. Thompson, *J. Chem. Phys.* **70**, 2748 (1979).

⁷C. Kubach, C. Courbin-Gaussorgues, and V. Sidis, *Chem. Phys. Lett.* **119**, 523 (1985).

⁸A. Russek and R. J. Furlan, *Phys. Rev. A* **39**, 5034 (1989); R. J. Furlan, G. Bent and A. Russek, *J. Chem. Phys.* **93**, 6676 (1990); R. J.

Furlan and A. Russek, *Phys. Rev. A* **42**, 6436 (1990).

⁹P. J. Kuntz, *Chem. Phys. Lett.* **16**, 581 (1972); W. N. Whitton and P. J. Kuntz, *J. Chem. Phys.* **64**, 3624 (1976); *Chem. Phys. Lett.* **34**, 340 (1975).

¹⁰F. Schneider and L. Zulicke, *Chem. Phys. Lett.* **67**, 491 (1979); R. Polak, J. Vojtik, I. Paidareva, and F. Schneider, *Chem. Phys.* **55**, 183 (1981); **76**, 259 (1983).

¹¹T. O. Tiernan and C. Lifshitz, *Adv. Chem. Phys.* **45**, 81 (1981).

¹²N. Sathyamurthy, *Chem. Phys.* **62**, (1981); T. Joseph and N. Sathyamurthy, *J. Chem. Phys.* **80**, 5332 (1984); *J. Indian Chem. Soc.* **62**, 874 (1985); N. Sathyamurthy, M. Baer, and T. Joseph, *Chem. Phys.* **114**, 73 (1987).

¹³S. H. Sucksalk and R. W. Emmons, *Phys. Rev. A* **29**, 2906 (1984).

¹⁴T. Joseph and N. Sathyamurthy, *J. Chem. Phys.* **86**, 704 (1987).

¹⁵E. A. Gislason and P.-M. Guyon, *J. Chem. Phys.* **86**, 677 (1987); M. Sizun, G. Parlant, and E. A. Gislason, *ibid.* **88**, 4294 (1988); M. Sizun and E. A. Gislason, *ibid.* **91**, 4603 (1989).

¹⁶J. D. Kress, R. B. Walker, and E. F. Hayes, *J. Chem. Phys.* **93**, 8085 (1990).

¹⁷J. Z. H. Zhang, D. L. Yeager, and W. H. Miller, *Chem. Phys. Lett.* **173**, 489 (1990).

¹⁸B. Lepetit and J. M. Launay, *J. Chem. Phys.* **95**, 5159 (1991).

¹⁹A. Aguado and M. Paniagua, *J. Chem. Phys.* **96**, 1265 (1992).

²⁰A. J. C. Varandas, *Adv. Chem. Phys.* **74**, 255 (1988).

²¹R. Rydberg, *Z. Phys.* **73**, 25 (1931).

²²R. K. Preston and D. L. Thompson, *J. Chem. Phys.* **68**, 13 (1978).

²³B. H. Mahan, *J. Chem. Phys.* **55**, 1436 (1971); *Acc. Chem. Res.* **8**, 55 (1975).

²⁴M. Dini, *Tesi di Laurea, Proprietà delle Superfici di Energia Potenziale e Reattività Chimica dei Sistemi M+HX* (Università di Perugia, 1985); A. Laganà, M. Dini, E. García, J. M. Alvaríño, and M. Paniagua, *J. Phys. Chem.* **95**, 8379 (1991).

²⁵G. Hirsch, R. J. Buenker, and C. Petrongolo, *Mol. Phys.* **70**, 835 (1990).

²⁶G. J. Atchity, S. S. Xantheas, and K. Ruedenberg, *J. Chem. Phys.* **95**, 1862 (1991).

²⁷S. Carter and J. N. Murrell, *Mol. Phys.* **41**, 567 (1980).

²⁸J. N. Murrell, S. Carter, I. M. Mills, and M. F. Guest, *Mol. Phys.* **42**, 605 (1981).

²⁹N. Sathyamurthy, *Comp. Phys. Rep.* **3**, 1 (1985).